De Novo Ligand Design: Understanding Stereoselective Olefin Binding to $[(\eta^5\text{-}C_5H_5)Re(NO)(PPh_3)]^+$ with Molecular Mechanics, Semiempirical Quantum Mechanics, and Density Functional Theory

Aaron M. Gillespie, Glenn R. Morello, and David P. White*

Department of Chemistry, University of North Carolina at Wilmington, 601 South College Road, Wilmington, North Carolina 28403-3297

Received May 13, 2002

Understanding stereoselective prochiral α-olefin binding by a chiral organometallic moiety is essential to control the production of a desired stereoisomer. Computational methods are useful predictors of stereoisomers, if all conformations that can participate in a reaction are identified. Herein we report a combined molecular mechanics, semiempirical quantum mechanics, and density functional theory study of binding of CH_2═CHR, R = Me, *n*-Pr, CH_2Ph, Ph, *i*-Pr, *t*-Bu, $SiMe_3$, to chiral $[(\eta^5\text{-}C_5H_5)Re(NO)(PPh_3)]^+$. In agreement with the experimental literature and previous computational results, one isomer was predicted to form preferentially over others. Brown's ligand repulsive energy was used to quantify the steric demand of the α-olefin in the organorhenium environment. A new conformational searching method, which requires successive applications of molecular mechanics, semiempirical quantum mechanics, density functional theory, restricted molecular mechanics, and density functional theory is introduced in order to identify *all conformational minima* that can participate in a reaction. A computationally derived diastereoselective excess based on DFT computations is derived and compared with experiment.

Introduction

Designing catalysts to carry out controlled stereoselective transformations is an important goal in contemporary computational organometallic chemistry. Several important catalytic pathways have been modeled with molecular mechanics (MM), semiempirical quantum mechanics (SEQM), and ab initio (mostly DFT) methods.[1−5] The foundation of a good computational model of an experimental system is a thorough conformational search. The chemical diversity of the transition metals, which makes them such versatile catalysts, presents the major challenge for the development of a de novo structural prediction protocol. Any de novo computational model of an organometallic complex must take into account five possible levels of isomerization:[6,7](i) geometric isomers (e.g., *mer* versus *fac* for octahedral complexes), (ii) structural isomers (e.g., octahedral versus trigonal prismic for six-coordinate complexes), (iii) coordination isomers (e.g., basal versus apical for octahderal complexes), (iv) linkage isomers (e.g., cyanide versus isocyanide), and (v) spin "isomers" (typically for open-shell d^2−d^8 metal ions).

There are three accepted strategies for conformational searching in inorganic chemistry:[8] grid searches, stochastic searches, and applications of molecular dynamics. In stochastic searches, the user determines how many total conformers are produced, which is potentially problematic since there is no guarantee that *all* important conformers are discovered. The conformational spaces of metals that are part of chelate ring systems are particularly difficult to sample, and to our knowledge, LIGB is the only stochastic search that is capable of changing chelate ring conformation.[6] During an LIGB search, all "ligand bonds", designated by the user, are broken and all torsion angles in the molecule, including those generated by the broken bonds, are rotated by randomly different amounts.[6] Prior to geometry optimization, the ligand bonds are reattached. Combination of LIGB and high-temperature molecular dynamics is an efficient method for searching the conformational space of a transition-metal-containing complex.

Low-temperature molecular dynamics (LTMD, temperatures around 500 K) is frequently used to refine a minimum. If the potential energy surface of a molecule contains several minima of similar energies separated

* To whom correspondence should be addressed at aaiPharma, Inc. 2320 Scientific Park Drive, Wilmington, NC 28405. E-mail: David.White@aaiPharma.com.

(1) Burkert, U.; Allinger, N. L. *Molecular Mechanics*; ACS Monograph 177; American Chemical Society: Washington, DC, 1982.
(2) Rappé, A. K.; Casewitt, C. J. *Molecular Mechanics Across Chemistry*; University Science Books: Sausalito, CA, 1997.
(3) Comba, P.; Hambley, T. W. *Molecular Modeling of Inorganic Compounds*, 2nd ed.; Wiley-VCH: Weinheim, Germany, 2001.
(4) Cundari, T. R., Ed. *Computational Organometallic Chemistry*; Marcel Dekker: New York, 2001.
(5) Jensen, F. *Introduction to Computational Chemistry*; Wiley: New York, 1999.
(6) Buda, C.; Burt, S. K.; Cundari, T. R.; Shenkin, P. S. *Inorg. Chem.* **2002**, *41*, 2060−2069.
(7) Ball, D. M.; Buda, C.; Gillespie, A. M.; Cundari, T. R.; White, D. P. *Inorg. Chem.* **2002**, *41*, 152−156.
(8) Bartol, J.; Comba, P.; Melter, M.; Zimmer, M. *J. Comput. Chem.* **1999**, *20*, 1549−1558.

10.1021/om020386h CCC: $22.00
Publication on Web 08/16/2002

by low energy barriers, then LTMD will locate the lowest energy minimum. High-temperature molecular dynamics (HTMD, $T > 750$ K), on the other hand, will provide the system with sufficient energy to rotate phenyl rings, for example. Cundari has shown that a combination of LIGB and HTMD is a good strategy to locate important minima in organometallic complexes.[6] Work from our group has indicated that a combination of stochastic conformational search and LTMD provides a good representation of the lowest energy structure for a complex.[9−12] Most conformational searches on organometallic complexes are carried out in molecular mechanics because of the relatively large number of basis functions and the number of structures that need to be generated to adequately sample the conformational space. Steric effects are well represented in MM;[1] therefore, the conformational search results are a good indication of the steric map of metal-containing complexes.

Several important catalytic reactions are thought to be dominated by steric effects. For example, Gladysz has demonstrated that chirally pure, coordinatively unsaturated $[(\eta^5\text{-}C_5H_5)Re(NO)(PPh_3)]^+$ fragments can stereospecifically bind prochiral unsaturated moieties and postulated that the sterically demanding ligands direct the substituents on the unsaturated moiety into the least congested interstice between ligands.[13] To test the hypothesis that steric effects govern the chiral recognition abilities of $[(\eta^5\text{-}C_5H_5)Re(NO)(PPh_3)]^+$, we have used Brown's ligand repulsive energy methodology[14] to determine which isomer of $[(\eta^5\text{-}C_5H_5)Re(\eta^2\text{-}$unsaturated moiety$)(NO)(PPh_3)]^+$ is the most *sterically accessible*.[9]

Ligand repulsive energy is the amount of nonbonded repulsion between a ligand and its environment.[14] Consider the case of a ligand, L, attached to a prototypical $Cr(CO)_5$ environment in its lowest energy form, either computed from molecular mechanics, semiempirical quantum mechanics, DFT methods or obtained from experiment such as an X-ray structure.[9−12,14−19] To compute ligand repulsive energy, E_R, for L, the van der Waals term is changed from the Buckingham potential

$$E_{vdW} = D_0\left\{\left[\left(\frac{6}{\gamma-6}\right)\exp\left[\gamma\left(1-\frac{r}{r_0}\right)\right]\right]-\left(\frac{\gamma}{\gamma-6}\right)\left(\frac{r_0}{r}\right)^6\right\} \quad (1)$$

to the pure repulsive form

$$E_{vdW}{}^{Rep} = D_0\exp\left\{\gamma\left(r_0-\frac{r}{r_0}\right)\right\} \quad (2)$$

In eqs 1 and 2, D_0 is the depth of the van der Waals well, γ is a scaling factor, r_0 is the van der Waals radius of the atom, and r is the internuclear distance. The ligand repulsive energy is then given by

$$E_R = -r_e\left(\frac{\partial E_{vdW}{}^{Rep}}{\partial r}\right) \quad (3)$$

where r_e is the equilibrium Cr−donor atom distance and $E_{vdW}{}^{Rep}$ is the van der Waals repulsive energy defined in eq 2. As the Cr−donor atom distance, r, changes, the amount of nonbonded repulsion between ligand and environment also changes. The negative sign in eq 3 ensures that E_R increases as the ligand gets more bulky.[14,17] Our group has produced a piece of code, ERCODE, that automates the calculation of ligand repulsive energies.[12]

In previous papers, we demonstrated that ligand repulsive energies were internally consistent, whether they were generated from molecular mechanics input structures or semiempirical quantum mechanics input structures.[9,19] Moreover, the same trends in ligand repulsive energies were found from both sets of input structures.

A previous application of molecular mechanics to understanding stereoselective binding of prochiral α-olefins to chiral $[(\eta^5\text{-}C_5H_5)Re(NO)(PPh_3)]^+$ fragments revealed that the lowest energy isomer with the olefin in the least sterically congested environment is the one that dominates in the experimental reaction.[9] A computationally derived diastereoselective excess, de_{MM}, was able to correctly predict the preferred face of the olefin bound to Re.

Semiempirical quantum mechanics (SEQM) was subsequently used to refine the MM-optimized geometries of $[(\eta^5\text{-}C_5R_5)Re(\eta^2\text{-}$unsaturated moiety$)(NO)(L)]^+$ (R = H, Me; L = PMe_3, PPh_3).[19] Ligand repulsive energies for the olefins in the SEQM-optimized environments were computed and again revealed that the experimentally observed major isomers were also the favored isomers predicted by SEQM.[19] Finally, the SEQM-based diastereoselective excess, de_{SEQM}, was linearly related to total cone angle of all ligands in $[(\eta^5\text{-}C_5R_5)Re(\eta^2\text{-}$unsaturated moiety$)(NO)(L)]^+$.[19]

In this paper we report the full de novo ligand design model for the recognition of prochiral olefins by $[(\eta^5\text{-}C_5H_5)Re(NO)(PPh_3)]^+$. Specifically, this paper addresses the problems of (i) full conformational space sampling of both organometallic fragment and prochiral substrate, (ii) quantification of the steric interaction between fragment and substrate, (iii) appropriate energy computation for each isomer of the substrate bound to the fragment, and (iv) derivation of a meaningful energy-weighted quantitative steric measure for each important isomer. In all cases, the organometallic model consists of $[(\eta^5\text{-}C_5H_5)Re(NO)(PPh_3)]^+$ bound to a series of prochiral α-olefins, $CH_2{=}CHR$ (R = Me, *n*-Pr, CH_2Ph, Ph, *i*-Pr, *t*-Bu, $SiMe_3$), for which experimental selectivities are known.[13]

Computational Methods

Molecular mechanics calculations were carried out with Cerius^2 4.5 available from Accelrys[20] with the Universal Force

(9) Gillespie, A. M.; White, D. P. *Organometallics* **2001**, *20*, 5149−5155.
(10) White, D. P.; Brown, T. L. *Inorg. Chem.* **1995**, *34*, 2718−2724.
(11) White, D. P.; Anthony, J. C.; Oyefeso, A. O. *J. Org. Chem.* **1999**, *64*, 7707−7716.
(12) Bubel, R. J.; Douglass, W.; White, D. P. *J. Comput. Chem.* **2000**, *21*, 239−246.
(13) Gladysz, J. A.; Boone, B. J. *Angew. Chem., Int. Ed. Engl.* **1997**, *36*, 550−583.
(14) Brown, T. L. *Inorg. Chem.* **1992**, *31*, 1286−1294.
(15) Choi, M.-G.; Brown, T. L. *Inorg. Chem.* **1993**, *32*, 1548−1553.
(16) Choi, M.-G.; Brown, T. L. *Inorg. Chem.* **1993**, *32*, 5603−5610.
(17) Choi, M.-G.; White, D.; Brown, T. L. *Inorg. Chem.* **1994**, *33*, 5591−5594.
(18) White, D. P. In *Computational Organometallic Chemistry*; Cundari, T. R., Ed.; Marcel Dekker: New York, 2001, pp 39−69.
(19) Gillespie, A. M.; White, D. P. *Internet Electron. J. Mol. Des.* **2002**, *1*, 23−36, http://www.biochempress.com.

Field.[21] Semiempirical calculations were carried out with Spartan 5.1 available from Wavefunction,[22] in which the PM3-(tm) Hamiltonian was genetics algorithm (GA) optimized for prediction of geometries.[23] Dmol^3 was used for DFT calculations[24] with the BOP functional[25] and VPSR relativistic pseudopotential.[26] Since Re is a third-row transition metal, relativistic effects must be accounted for. To account for relativistic effects, and obtain optimized structures in an expedient quantity of time, the VPSR relativistic pseudopotential was employed. A double-numeric basis set with polarization functions was used for geometry optimization, and a double-numeric basis set with double polarization functions was used for single-point energy calculations. We abbreviate the computation with BOP functional with double-numeric basis set with polarization functions as BOP/DNP and with double-polarization functions as BOP/DNPP. Conformational searches for the olefin, $[(\eta^5\text{-}C_5H_5)Re(NO)(PPh_3)]^+$ fragment, and $[(\eta^5\text{-}C_5H_5)Re(\eta^2\text{-}CH_2{=}CHR)(NO)(PPh_3)]^+$ were performed as reported previously, unless otherwise noted.[9]

Results and Discussion

De Novo Ligand Design. Cundari has recently noted that optimal ligand design requires the use of many levels of computational theory rather than the traditional approach of using just one level of theory for a given problem.[6,7] Each computational level of theory provides a more sophisticated refinement than its predecessor. The Cundari strategy is different from the ONIOM methodology, in which different levels of computational theory are applied to different portions of the same molecule.[27−29] In Cundari's de novo design approach, each successive methodology is increasingly computationally expensive from MM through SEQM to DFT. Because of this increase in computation time, fewer structures can be submitted at each successive level of theory in order for the computations to be completed expediently. Therefore, Cundari has designed a pyramid approach during which MM, SEQM, and DFT methods are used in sequence on an increasingly smaller set of structures (Figure 1).

In the de novo ligand design approach, MM is used to sample the gross conformational space of the molecule. High-energy MM conformers are eliminated on steric grounds, which are well represented in MM.[1] Selected low-energy MM structures are submitted to SEQM for accurate *geometry prediction*. Although SEQM energies are not always reliable measures of heats of formation, the PM3(tm) level of theory is capable of predicting accurate geometries for organometallic species.[6,30] Consequently, the geometry that results from SEQM optimization is an excellent starting point for the DFT computation. In a benchmark test during this study, the MM-optimized structure was used as the starting point for the BOP/DNP optimization, which resulted in convergence times up to 7 times slower than when the SEQM-optimized geometry was used as the starting point in the DFT computation.

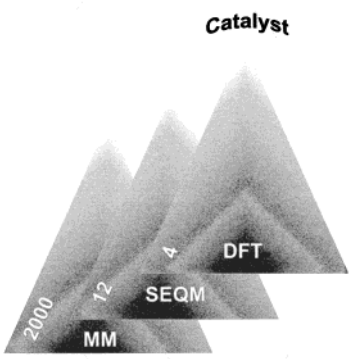

Figure 1. De novo design pyramid illustrating the successive applications of more sophisticated computational methods in order to refine a catalyst structure.

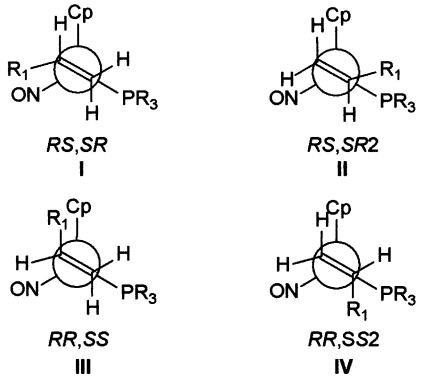

Figure 2. Four isomers of $[(\eta^5\text{-}C_5H_5)Re(\eta^2\text{-}$prochiral olefin$)(NO)(PPh_3)]^+$. Structures **I** and **II** have the same olefinic face bound to the Re, as do isomers **III** and **IV**.

Both geometric refinement and accurate energy determination in the de novo scheme occur with quantum-mechanical methods. For organometallic species with a large number of basis functions, DFT is usually the quantum-mechanical method of choice.[4]

There are four different isomers generated when a prochiral olefin can bind to a $[(\eta^5\text{-}C_5H_5)Re(NO)(PPh_3)]^+$ fragment, shown as **I**−**IV** in Figure 2. Gladysz has suggested, and we have demonstrated, that the *RS*,*SR* isomer contains the olefinic substituents in the least congested environment relative to the ligand set.[9,13] In the study reported here, DFT computations are performed on four isomers (Figure 2) per olefin in order to meaningfully assess the diastereoselectivity of the system. Prior to DFT computation, MM is used to produce 2000 conformers per isomer **I**−**IV**;[9] the lowest energy of each isomer is passed onto SEQM[23] for accurate geometry optimization. Finally, these four structures are then submitted to DFT (BOP/DNP and then BOP/DNPP) for accurate energy computation.

To compare the computed results with experiment, the CSD was searched for high-quality (R < 10%), monomeric crystal structures with no reported error and no crystallographic disorder.[31] As anticipated, both SEQM and BOP/DNP structures agree well with struc-

(20) Cerius^2 4.5; Accelrys, Inc., San Diego, CA, 2001.
(21) Rappé, A. K.; Casewit, C. J.; Colwell, K. S.; Goddard, W. A., III; Skiff, W. M. *J. Am. Chem. Soc.* **1992**, *114*, 10024−10035.
(22) Wavefunction, Inc. 18401 von Karman Avenue, Suite 370, Irvine, CA 92612.
(23) Cundari, T. R.; Deng, J.; Fu, W. *Int. J. Quantum Chem.* **2000**, *77*, 421−432.
(24) Delley, B. *J. Phys. Chem.* **1990**, *92*, 508−517.
(25) Tsuneda, T.; Suzumura, T.; Hirao, K. *J. Chem. Phys.* **1999**, *110*, 10664−10678.
(26) Delley, B. *Int. J. Quantum Chem.* **1998**, *69*, 423.
(27) Svenson, M.; Humbel, S.; Froese, R. D. J.; Matsubara, T.; Sieber, S.; Morokuma, K. *J. Phys. Chem.* **1996**, *100*, 19357.
(28) Dapprich, S.; Komáromi, I.; Byun, K. S.; Morokuma, K.; Frisch, M. J. *J. Mol. Struct. (THEOCHEM)* **1999**, *461*, 21.
(29) Maseras, F. In *Computational Organometallic Chemistry*; Cundari, T. R., Ed.; Marcel Dekker: New York, 2001; pp 159−184.
(30) Cundari, T. R.; Fu, W. *Inorg. Chim. Acta* **2000**, *300*−*302*, 113.

Table 1. Comparison of Experimental and Computed Bond Distances (Å), Angles (deg), and Torsion Angles (deg) for [(η^5-C_5H_5)Re(η^2-α-olefin)(NO)(PPh_3)]$^+$ Complexes Generated with MM, SEQM, and DFT (BOP/DNP) Methods

bond or angle	X-ray[31]	no. of data points in CSD	MM structure[9]	SEQM structure[19]	DFT structure
Re−Cp(centroid)	1.95(3)	199		2.00(1)	2.05(1)
Re−Cp ring C	2.29(4)	199	2.04(9)		
Re−P	2.43(5)	1806	2.53(1)	2.47(1)	2.53(1)
Re−N	1.76(4)	207	1.992(1)	1.81(2)	1.781(2)
Re−CH_2(olefin)	2.24(7)	56	2.00(4)	2.08(1)	2.26(2)
Re−C_{ipso}(olefin)	2.26(10)	56	2.28(4)	2.10(2)	2.34(4)
Re−C(olefin centroid)	2.13(8)	56	2.04(2)	1.95(1)	2.19(2)
N−O	1.19(3)	207	1.10	2.204(2)	1.193(1)
C═C	1.41(4)	56	1.389(1)	1.499(3)	1.427(4)
Re−N−O	174(3)	207	179.3(4)	169(2)	172(2)
Re−C(olefin centroid)−C_{ipso}	91(1)	9		90.8(9)	94(2)
Re−C(olefin centroid)−C_{ipso}−P	−2(16)	9		−175(2), 9(5)	−172(4), 9(5)

tural parameters obtained from the CSD (Table 1). As the computational method becomes more sophisticated (MM to SEQM to DFT), the olefin becomes more orthogonal to the Re−centroid vector, as evidenced in the Re−C(olefin) bond distances (Table 1; 0.02 Å difference in the crystal structures,[31] 0.28 Å difference by MM, 0.02 Å difference by PM3(tm), and 0.08 Å by BOP/DNP). The Re−nitrosyl interaction (Re−N distance and Re−N−O angles) is modeled well with BOP/DNP but less so with PM3(tm). Conversely, the Re−Cp interaction is better modeled with PM3(tm) than with BOP/DNP (Table 1). Finally, the olefinic C═C bond eclipses the Re−P bond vector (Re−C(olefin centroid)−C_{ipso}−P torsion angles of −175(2)/+9(5)° by PM3(tm) and −172(4)/9(5)° by BOP/DNP). This eclipsing of the olefinic C═C bond with the Re−P bond vector is thought to optimize the overlap between filled Re d-orbitals and olefinic π*-orbitals.[13] The negative torsion angles result from rotamers **I** and **III** in Figure 2.

Steric Size of the Olefin in the [(η^5-C_5H_5)Re(NO)(PPh_3)]$^+$ Environment Computed from SEQM and DFT Structures. Work from our laboratories, as well as Brown's, has suggested that any good representation of the structure of an organometallic complex is an acceptable starting point for a ligand repulsive energy calculation.[10−12] We have shown that the *trend in ligand repulsive energy* does not depend significantly on the prototypical fragment used for the calculation.[10−12,15−17] We have also shown that ligand repulsive energies do not depend greatly on the force field employed for their computation.[12] In this paper, we now address the question of whether ligand repulsive energies determined from MM-, SEQM-, or DFT-optimized structures are comparable. It is important to note, that ligand repulsive energies are always computed from eq 3 and that SEQM- and DFT-optimized structures are merely the input files. Ligand repulsive energies were computed with ERCODE, which was developed in our laboratories.[12]

Plots of ligand repulsive energy from the MM or SEQM structure against ligand repulsive energy from the DFT structure are linear and almost parallel with a 10 kcal/mol difference in intercepts (Figure 3). The small amount of scatter in the plots is mostly likely due to conformational effects (see below). We may conclude that the ligand repulsive energy methodology provides a robust, quantitative measure of steric effects invariant to prototypical fragment, MM force field, or level of theory used to derive the starting structure.

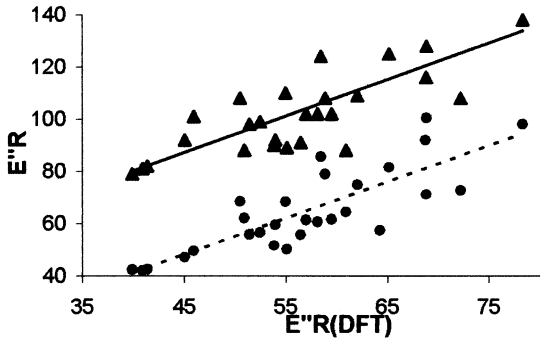

Figure 3. Plots of ligand repulsive energy, E''_R, from MM-optimized structures (triangles) and SEQM-optimized structures (circles) versus E''_R computed from the DFT-optimized structure.

DFT Model of Stereoselective Binding of Prochiral α-Olefins to [(η^5-C_5H_5)Re(NO)(PPh_3)]$^+$. All the lowest energy conformers generated from the SEQM study[19] were submitted to Dmol^3 for geometry optimization with the BOP functional with a double-numeric basis set with polarization functions (BOP/DNP) and the VPSR relativistic pseudopotential.[24−26] Single-point energies were computed for the BOP/DNP-optimized structures with a double-numeric basis set with double polarization functions (BOP/DNPP). The BOP/DNP-optimized structures were submitted to ERCODE for ligand repulsive energy computation. The DFT and ERCODE results are summarized in Table 2.

To ensure the BOP functional[25] provides consistent results, single-point energy calculations with DNPP basis set were performed on all isomers of [(η^5-C_5H_5)-Re(η^2-CH_2═CHR)(NO)(PPh_3)]$^+$, R = Me, *i*-Pr, Bn (Figure 2), with the BLYP[32,33] and BP[32,34] functionals in Dmol^3.[24] In addition, single-point energies were computed for the [(η^5-C_5H_5)Re(η^2-CH_2═CHMe)(NO)(PPh_3)]$^+$ complex with the B3LYP[33,35] functional in Gaussian 98.[36] Energies relative to the lowest energy isomer for a given olefin are tabulated in Table 3. There is good agreement between the relative energies of the isomers

(31) Allen, F. H.; Kennard, O. *Chem. Des. Autom. News* **1993**, *8*, 31−37.

(32) Becke, A. D. *Phys. Rev., B* **1988**, *38*, 3098.

(33) Lee, C.; Yang, W.; Parr, R. G. *Phys. Rev., B* **1988**, *37*, 785−789.

(34) Perdew, J. P.; Chevary, J. A.; Vosko, S. H.; Jackson, K. A.; Peterson, M. R.; Singh, D. J.; Fiolhais, C. *Phys. Rev., B* **1992**, *46*, 6671.

(35) Becke, A. D. *J. Chem. Phys.* **1992**, *98*, 5648−5652.

Table 2. Single-Point BOP/DNPP Energies (in kcal/mol) Relative to the Lowest Energy Isomer and Ligand Repulsive Energies, $E''_R{}^{DFT}$ (kcal/mol), for the α-Olefins in the $[(\eta^5\text{-}C_5H_5)Re(NO)(PPh_3)]^+$ Environment

olefin substituent	isomer (Figure 2)	rel BOP/DNPP energy	$E''_R{}^{DFT}$
Me	*RS,SR*	0	39.9
	*RS,SR*2	3.636	51.4
	RR,SS	2.858	55.1
	*RR,SS*2	6.112	56.4
Bn	*RS,SR*	0	40.9
	*RS,SR*2	4.727	50.9
	RR,SS	2.723	53.8
	*RR,SS*2	6.426	59.5
i-Pr	*RS,SR*	0	54.0
	*RS,SR*2	3.655	50.5
	RR,SS	2.779	57.0
	*RR,SS*2	5.477	68.8
Ph	*RS,SR*	0	45.9
	*RS,SR*2	4.388	68.8
	RR,SS	0.634	65.2
	*RR,SS*2	7.633	57.6
n-Pr	*RS,SR*	0	41.4
	*RS,SR*2	9.101	55.0
	RR,SS	6.31	60.9
	*RR,SS*2	6.586	58.1
t-Bu	*RS,SR*	0	52.4
	*RS,SR*2	10.239	68.9
	RR,SS	7.108	72.2
	*RR,SS*2	12.854	78.3
$SiMe_3$	*RS,SR*	0	45.1
	*RS,SR*2	6.445	58.5
	RR,SS	5.362	62.0
	*RR,SS*2	13.135	58.9

Table 3. Single-Point DFT/DNPP Energies (kcal/mol) Relative to the Lowest Energy Isomer Computed for Different Functionals

olefin substituent	isomer (Figure 2)	energy			
		B3LYP	BLYP	BP	BOP
Me	*RS,SR*	0	0	0	0
	*RS,SR*2	3.576	3.838	3.849	3.636
	RR,SS	3.438	2.102	3.014	2.858
	*RR,SS*2	5.255	5.382	6.228	6.112
Bn	*RS,SR*		0	0	0
	*RS,SR*2		4.369	4.862	4.727
	RR,SS		1.275	2.789	2.723
	*RR,SS*2		5.459	6.608	6.426
i-Pr	*RS,SR*		0	0	0
	*RS,SR*2		3.947	4.390	3.655
	RR,SS		3.022	2.738	2.779
	*RR,SS*2		6.906	5.573	5.477

across the functionals studied. In all cases, the *RS,SR* isomers have the lowest BOP/DNPP energies, in agreement with Gladysz's hypothesis and our previous results.[9,13,19]

Single-point BOP/DNPP energies for the BOP/DNP-optimized structures are shown in Table 2. These energies are reported relative to the lowest energy structure for each olefin. As anticipated, the *RS,SR* isomers all have the lowest energies.[9,13,19] With the exception of the 1-butene ligand, the energies of the isomers increase as *RS,SR* > *RR,SS* > *RS,SR*2 > *RR,SS*2 (Table 2).[9,13,19] This energy trend is expected on the basis of the simple rationalization that the energy of an isomer increases as the substituent on the α-olefin interacts with the sterically demanding ligands on Re.[9,13,19] The propyl substituent in the 1-butene ligand is responsible for the break in energy trend, which is an indication of a potential problem in the conformational search strategy employed.

Computational Measure of Diastereoselectivity, de. (a) Conformational Searching. In order for a complex to efficiently participate in the stereoselective binding of a prochiral olefin, two conditions must be satisfied: (i) one isomer must have a lower energy than the others and (ii) one isomer must contain the olefin in a less sterically congested environment than the others. Condition i is met when an isomer has a low BOP/DNPP energy, whereas condition ii is met when one isomer has a low E''_R value.

In previous papers in this series, we reported MM and SEQM results that enabled us to rationalize prochiral olefin binding using a purely steric model.[9,19] These results assumed that only one conformer per isomer dominated in the recognition of the prochiral olefin (Figure 2). However, diastereoselectivities (see below) computed on olefins with conformationally flexible substituents did not agree with experiment. This prompted the question of whether certain important conformers were missing from consideration.

Combined QM/MM methods assume that the reaction center of a molecule can be treated with quantum mechanics while the conformationally flexible, "steric", portions can be treated with molecular mechanics, affording meaningful results in a modest amount of time.[29] Therefore, to locate any missing minima, we undertook a modified MM/DFT approach.

Each BOP/DNP-optimized isomer was imported from Dmol[3] into Cerius[2], and all atom positions were frozen except those atoms in the substituent on the olefin. The conformational space of the substituent on the olefin was explored by means of a grid search, and each resulting conformer was partially energy minimized with the UFF (only the atoms in the substituents were geometry optimized).[21] The torsion angle window was set from −90 to +90° for substituents with a C_2 axis and −180 to +180° for substituents with a pseudo C_3 axis of symmetry. The grid was set to 1 or 10°, depending on the total number of conformers generated (for example, a 1° grid was used for structures with only one rotatable bond, whereas a 10° grid was used for the $[(\eta^5\text{-}C_5H_5)Re\{\eta^2\text{-}CH_2{=}CH(n\text{-}Pr)\}(NO)(PPh_3)]^+$ isomers). The results for the grid search on the *RS,SR*2 isomer for $[(\eta^5\text{-}C_5H_5)Re\{\eta^2\text{-}CH_2{=}CH(n\text{-}Pr)\}(NO)(PPh_3)]^+$ are shown in Figure 4. (The isomer labels in Figure 4 are shown in Table 4.) There are several redundant minima in Figure 4; for example, the data point at **A**(180, 180°) is the same as (**A**)(−180, −180°), (**A**)(−180, 180°), etc. These redundancies are indicated by placing the isomer label in parentheses. The minimum at approximately (180, −60°) was found to converge to A after full BOP/DNP geometry optimization.

(36) Frisch, M. J.; Trucks, G. W.; Schlegel, H. B.; Scuseria, G. E.; Robb, M. A.; Cheeseman, J. R.; Zakrzewski, V. G.; Montgomery, J. A., Jr.; Stratmann, R. E.; Burant, J. C.; Dapprich, S.; Millam, J. M.; Daniels, A. D.; Kudin, K. N.; Strain, M. C.; Farkas, O.; Tomasi, J.; Barone, V.; Cossi, M.; Cammi, R.; Mennucci, B.; Pomelli, C.; Adamo, C.; Clifford, S.; Ochterski, J.; Petersson, G. A.; Ayala, P. Y.; Cui, Q.; Morokuma, K.; Malick, D. K.; Rabuck, A. D.; Raghavachari, K.; Foresman, J. B.; Cioslowski, J.; Ortiz, J. V.; Baboul, A. G.; Stefanov, B. B.; Liu, G.; Liashenko, A.; Piskorz, P.; Komaromi, I.; Gomperts, R.; Martin, R. L.; Fox, D. J.; Keith, T.; Al-Laham, M. A.; Peng, C. Y.; Nanayakkara, A.; Challacombe, M.; Gill, P. M. W.; Johnson, B. G.; Chen, W.; Wong, M. W.; Andres, J. L.; Gonzalez, C.; Head-Gordon, M.; Replogle, E. S.; Pople, J. A. *Gaussian 98*, revision A.9; Gaussian, Inc.: Pittsburgh, PA, 1998.

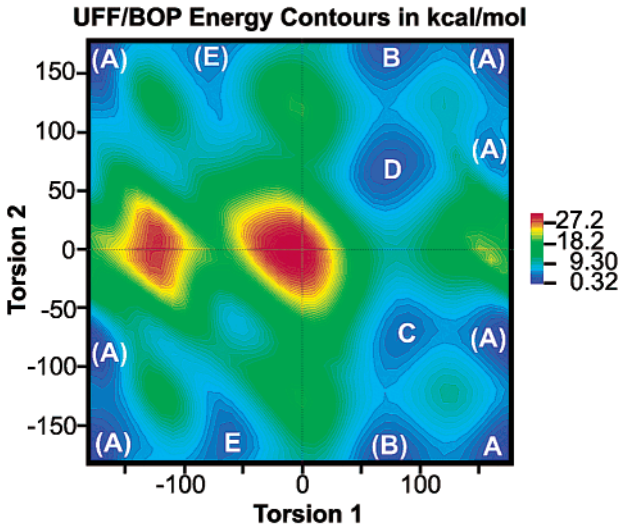

Figure 4. Grid search results on *RS,SR*2-[(η^5-C_5H_5)Re(η^2-1-butene)(NO)(PPh_3)]$^+$. The five low-energy unique isomers, **A**−**E** (Table 4), are generated by freezing all atoms in the molecule except those in the propyl substituent on the olefin. Redundant conformers are indicated in parentheses.

All potential minima from the grid search for [(η^5-C_5H_5)Re(η^2-CH_2=CHBn)(NO)(PPh_3)]$^+$ were submitted to Spartan and the structure geometries optimized under the same restraint as the MM structures (i.e., the BOP/DNP-optimized portion of the molecule was frozen). After SEQM optimization, many of the MM minima were found to be redundant. For example, the grid search found four minima for the *RS,SR* isomer, whereas SEQM only located two, one of which was not the global minimum found in the MM search. Although there is no guarantee that the lowest energy structure predicted with molecular mechanics is the same as the lowest energy structure predicted by SEQM, we were perturbed by the reduction of four MM minima to two SEQM minima. Furthermore, 16 of the 28 MM minima for the [(η^5-C_5H_5)Re{η^2-CH_2=CH(*i*-Pr)}(NO)(PPh_3)]$^+$ isomers did not converge in SEQM. Therefore, the SEQM step was skipped and the partially optimized MM structures were imported directly into Dmol^3 for full geometry optimization at the BOP/DNP level (Table 4; Figure 5).

Consider the **B** and **C** conformers of the *RS,SR* isomer for the benzyl substituent: the BOP/DNP energies are very similar, as are the torsion angles predicted by MM and determined by DFT. (Since there is a C_2 axis of symmetry about the phenyl ring of the benzyl substituent, a torsion angle of 65.4° is equivalent to 114.6°.) With Chem 3D Pro, these two structures were found to be superimposed with less than 0.1 RMS error and 0.01 RMS gradient. Therefore, we take these two conformers to be the same and conclude that the MM-predicted conformer with a C_{ipso}−CH_2−$C_{ipso(Ph)}$−C_{ortho} torsion angle of 64.4° is not an energy minimum according to the more sophisticated DFT level of theory. Similar analysis shows that conformers **A** and **B** of the *RS,SR*2 isomer for the *n*-Pr substituent are identical (Figures 5 and 6). All redundant conformers, defined by less than 0.1 RMS error and 0.01 RMS gradient in Chem 3D Pro, close torsion angles and close energies, are italicized in Table 4 are we not considered in any of the following analyses.

By restraining the BOP/DNP-optimized atomic positions in the immediate vicinity of the metal center in

Table 4. DFT (BOP/DNP) Optimized Energies (kcal/mol) Relative to the Lowest Energy Isomer for All Isomers of the [(η^5-C_5H_5)Re(η^2-CH_2=CHR)(NO)(PPh_3)]$^+$ Complexes Following Molecular Mechanics Grid Search and Torsion Angles (deg) for both the Partially UFF Optimized and Fully BOP/DNP Optimized Structures[a]

R	isomer (Figure 2)	isomer label	rel BOP/DNP energy	torsion angle predicted by MM 1	torsion angle predicted by MM 2	torsion angle found by DFT 1	torsion angle found by DFT 2
Bn	*RS,SR*	**A**	0.00	65.7	68.6	94.9	88.2
		B	0.23	−176.2	64.4	−168.2	115.5
		C	*0.38*	*−167.7*	*−71.9*	*−167.6*	*−65.4*
		D	4.40	−78.7	−85.6	95.0	−91.0
	*RS,SR*2	**A**	0.00	74.2	69.5	77.2	80.1
		B	0.56	161.7	−70.0	91.9	−59.9
		C	2.69	−78.0	87.1	−20.8	73.2
	RR,SS	**A**	0.00	−66.0	−68.3	−82.9	−77.6
		B	1.60	174.0	68.4	171.0	41.1
		C	3.67	77.0	−91.1	19.2	−68.4
	*RR,SS*2	**A**	0.00	97.8	−65.0	−79.8	−77.7
		B	0.04	−173.7	59.5	−89.8	45.3
		C	*0.16*	*−69.5*	*−68.3*	*−81.4*	*−82.5*
Ph	*RS,SR*	**A**	0.00	−68.2		−9.7	
		B	*0.01*	*65.0*		*−9.5*	
	*RS,SR*2	**A**	0.00	18.6		−13.6	
		B	*0.03*	*−90.0*		*−16.5*	
	RR,SS	**A**	0.00	−80.0		−173.2	
	*RR,SS*2	**A**	0.00	−70.0		−151.4	
i-Pr	*RS,SR*	**A**	0.00	−47.2		−38.2	
		B	2.54	174.0		−130.8	
		C	3.77	43.9		89.1	
	*RS,SR*2	**A**	0.00	−179.9		−153.6	
		B	1.85	−27.2		−41.9	
		C	2.61	−57.1		−67.7	
		D	4.98	107.5		58.2	
		E	*5.68*	*45.8*		*59.7*	
	RR,SS	**A**	0.00	51.6		45.7	
		B	0.24	132.6		137.3	
		C	3.71	−83.1		−85.9	
	*RR,SS*2	**A**	0.00	179.6		133.8	
		B	1.82	50.0		87.7	
		C	6.28	−45.6		−63.0	
n-Pr	*RS,SR*	**A**	0.00	70.7	178.3	90.6	−179.8
		B	1.17	−172.0	178.8	−166.4	−177.0
		C	1.18	66.0	66.7	86.5	66.8
		D	1.23	82.9	−72.9	94.7	−72.4
		E	2.45	−167.8	−74.3	−164.4	−69.5
		F	3.52	−80.5	179.0	−8.4	174.5
		G	*3.54*	*−87.9*	*−76.2*	*−9.9*	*178.6*
		H	4.52	−173.7	68.7	−179.4	84.2
		I	5.17	−91.5	84.1	−4.9	81.7
	*RS,SR*2	**A**	0.00	177.8	177.0	81.2	179.8
		B	*1.17*	*72.3*	*178.0*	*79.3*	*178.9*
		C	2.52	85.6	−71.4	88.6	−68.5
		D	2.61	71.2	69.1	75.2	72.6
		E	4.83	−61.8	−161.3	−25.9	177.4
	RR,SS	**A**	0.00	−70.8	−178.2	−92.8	179.9
		B	0.58	−160.3	−60.1	−93.3	−71.8
		C	*0.98*	*−65.7*	*−66.5*	*−88.7*	*−71.8*
		D	1.27	−83.2	72.9	−94.4	73.0
		E	2.74	173.7	−178.7	175.3	171.4
		F	*3.71*	*82.1*	*−168.3*	*3.2*	*−176.7*
		G	4.03	169.5	72.8	176.8	74.4
	*RR,SS*2	**A**	0.00	−72.3	−177.9	−77.5	−179.1
		B	*0.12*	*−158.7*	*−166.9*	*−81.8*	*179.2*
		C	1.09	−70.0	−70.0	−75.6	−69.4
		D	1.46	−160.0	80.0	−90.2	72.9
		E	*1.47*	*−84.8*	*72.0*	*−90.6*	*72.7*
		F	*1.50*	*174.1*	*59.9*	*−87.0*	*73.3*
		G	3.93	67.6	165.9	21.8	−174.0

[a] The highest energy structure for each redundant conformer is italicized.

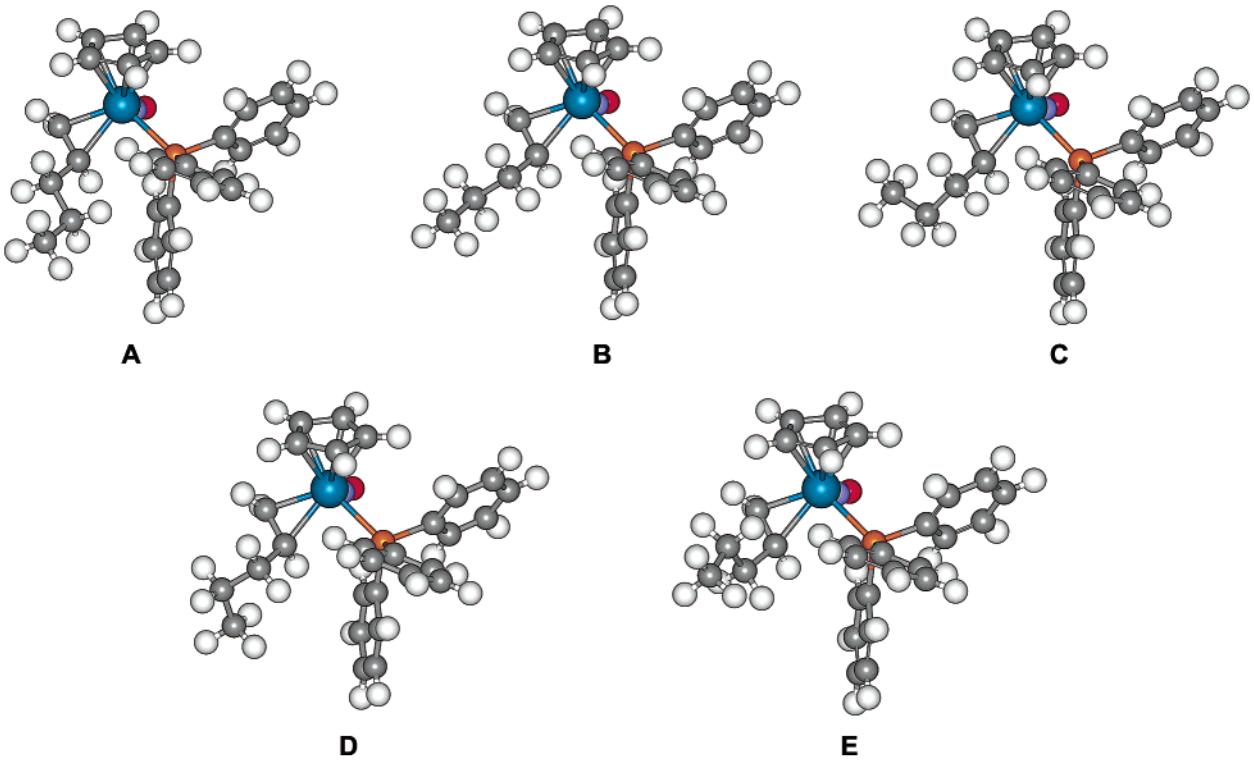

Figure 5. Five low-energy isomers, **A**−**E** (Table 4), generated from the DFT/MM conformational search on *RS*,*SR*2-[(η^5-C_5H_5)Re(η^2-1-butene)(NO)(PPh_3)]$^+$.

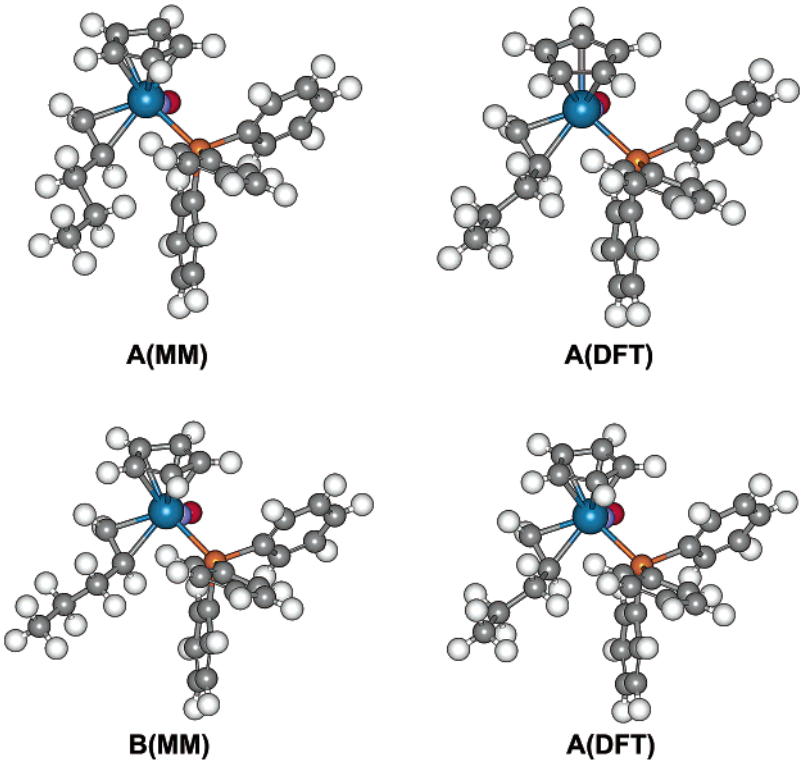

Figure 6. The two molecular mechanics minima, **A(MM)** and **B(MM)**, for *RS*,*SR*2-[(η^5-C_5H_5)Re(η^2-1-butene)(NO)(PPh_3)]$^+$ (Table 4), which collapse to a common minimum, **A(DFT)**, after optimization with BOP/DNP. Note that the conformation of the propyl substituent on the olefin is the same in **A(MM)** and **A(DFT)**.

the MM grid search, we mimic the ONIOM methodology.[27,28] However, reoptimization of the entire structure with BOP/DNP results in the finding that certain MM-predicted minima do not exist. If these minima are included in the computation of an energy-weighted property, then an incorrect result is highly likely. Therefore, an ONIOM type methodology is not appropriate for the system under investigation and the combined MM−SEQM−DFT−MM−DFT approach, illustrated in Figure 7, yields more accurate results.

It follows from our results that the initial MM conformational search is not as critical as we originally

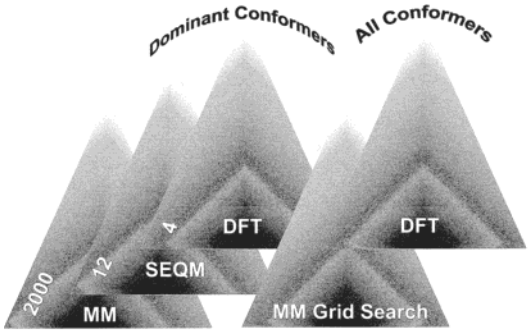

Figure 7. Modified de novo design pyramid illustrating the successive applications MM−SEQM−DFT−MM−DFT to identify all the conformers that can participate in the stereoselective olefin binding reaction.

Table 5. Molecular Mechanics Based Diastereoselectivities, de_{MM}, Based on All Unique Conformers Reported in Table 4 and Experimental Diastereoselective Excess Values, de,[13] for the Stereoselective Binding of α-Olefins to $[(\eta^5\text{-}C_5H_5)Re(NO)(PPh_3)]^+$

α-olefin	de_{MM}	de[13]
CH_2=CHMe	1.0	0.95
CH_2=CHBn	0.003	0.88
CH_2=CH(*i*-Pr)	0.11	0.99
CH_2=CHPh	1.0	0.93
CH_2=CH(*n*-Pr)	0.0	0.94
CH_2=CH(*t*-Bu)	1.0	0.73
CH_2=CHSiMe$_3$	1.0	0.63

predicted and significantly fewer structures are acceptable. The first SEQM step is still required in order to decrease the amount of computer time necessary for the convergence of the DFT jobs. The most critical part of the conformational search is the freezing of conformationally inflexible portions of the molecule in the DFT-optimized structure followed by a grid search performed on the olefinic substituent. The final set of hybrid DFT/MM minima requires full optimization by means of DFT methods, since MM is not sufficiently reliable to predict the final structure or energy of the system. If we are only interested in the lowest energy structure, then the original MM−SEQM−DFT approach is sufficient; however, if we need to identify *all minima* (see below) that can participate in a reaction, then the original MM−SEQM−DFT approach is not sufficient.

(b) Recomputed Diastereoselective Excess, de_{DFT}. In previous papers we introduced a computationally derived diastereoselective excess, de_{MM} and de_{SEQM}.[9,19] If ΔE_i is the relative BOP/DNPP energy of conformer i and kT = 0.592 476 141 388 kcal/mol at 298.15 K, then the Boltzmann weight of conformer i, w_i, is

$$w_i = \frac{\exp\left(-\frac{\Delta E_i}{kT}\right)}{\sum \exp\left(-\frac{\Delta E_i}{kT}\right)} \qquad (4)$$

We define the Boltzmann weighted ligand repulsive energy computed from the BOP/DNP optimized isomer for conformer i, $\langle E''_R\rangle_i$, as

$$\langle E''_R\rangle_i = w_i \exp\left(-\frac{\Delta E''_R}{kT}\right) \qquad (5)$$

Table 6. Ligand Repulsive Energies (kcal/mol) Computed from BOP/DNP Optimized Structures, E''_R, Boltzmann Weighted Ligand Repulsive Energies, $\langle E''_R\rangle$ (kcal/mol), Computed Diastereoselectivities, and Experimental Diastereoselectivities for the $[(\eta^5\text{-}C_5H_5)Re(\eta^2\text{-}CH_2$=$CHR)(NO)(PPh_3)]^+$ Complexes

R	isomer (Figure 2)	isomer label[a]	E''_R	$\langle E''_R\rangle$	de_{DFT}	de[13]
Me	*RS,SR*		39.9	1.0	0.99	0.95
	*RS,SR*2		51.4	7.7×10^{-12}		
	RR,SS		55.1	5.5×10^{-14}		
	*RR,SS*2		56.4	2.3×10^{-17}		
t-Bu	*RS,SR*		52.4	1.0	1.0	0.73
	*RS,SR*2		68.9	2.8×10^{-20}		
	RR,SS		72.2	1.9×10^{-20}		
	*RR,SS*2		78.3	4.0×10^{-29}		
$SiMe_3$	*RS,SR*		45.1	1.0	1.0	0.63
	*RS,SR*2		58.5	2.7×10^{-15}		
	RR,SS		62.0	4.2×10^{-17}		
	*RR,SS*2		58.9	1.8×10^{-20}		
Bn	*RS,SR*	**A**	40.5	0.4	0.81	0.88
		B	48.2	4.1×10^{-7}		
		D	40.5	0.4		
	*RS,SR*2	**A**	51.9	7.2×10^{-13}		
		B	58.1	6.3×10^{-18}		
		C	68.1	4.4×10^{-27}		
	RR,SS	**A**	52.9	3.9×10^{-12}		
		B	70.0	7.4×10^{-26}		
		C	64.8	10.0×10^{-24}		
	*RR,SS*2	**A**	55.5	5.7×10^{-17}		
		B	61.8	1.3×10^{-22}		
Ph	*RS,SR*	**A**	46.4	0.8	0.77	0.93
	*RS,SR*2	**A**	66.8	5.4×10^{-19}		
	RR,SS	**A**	64.2	2.1×10^{-14}		
	*RR,SS*2	**A**	62.0	7.4×10^{-18}		
i-Pr	*RS,SR*	**A**	45.7	1.0	0.99	0.99
		B	48.2	0.0		
		C	51.9	4.8×10^{-8}		
	*RS,SR*2	**A**	49.4	2.2×10^{-9}		
		B	51.0	7.4×10^{-12}		
		C	51.4	8.6×10^{-13}		
		D	59.8	1.1×10^{-20}		
	RR,SS	**A**	59.5	1.4×10^{-15}		
		B	55.0	1.5×10^{-12}		
		C	62.9	6.0×10^{-21}		
	*RR,SS*2	**A**	70.0	1.3×10^{-25}		
		B	63.7	3.5×10^{-22}		
		C	73.5	8.5×10^{-33}		
n-Pr	*RS,SR*	**A**	40.8	0.7	0.79	0.94
		B	42.4	0.0		
		C	41.8	0.0		
		D	40.9	0.1		
		E	43.9	6.7×10^{-5}		
		F	44.0	9.6×10^{-6}		
		H	43.9	1.8×10^{-6}		
		I	43.4	1.2×10^{-6}		
	*RS,SR*2	**A**	51.3	1.4×10^{-11}		
		C	51.0	2.3×10^{-13}		
		D	47.9	4.1×10^{-11}		
		E	56.4	5.4×10^{-19}		
	RR,SS	**A**	53.5	4.5×10^{-12}		
		B	53.7	1.0×10^{-12}		
		D	53.7	4.0×10^{-13}		
		E	61.5	6.2×10^{-20}		
		G	63.9	1.1×10^{-22}		
	*RR,SS*2	**A**	57.4	6.2×10^{-18}		
		C	57.8	4.5×10^{-19}		
		D	61.2	8.0×10^{-22}		
		G	64.6	3.9×10^{-26}		

[a] See Table 4.

where $\Delta E''_R$ is the relative ligand repulsive energy for isomer i. Finally, if $\langle E_{RS,SR}\rangle$ is the Boltzmann weighted ligand repulsive energy for the *RS,SR* isomer as defined in eq 5, $\langle E_{RS,SR2}\rangle$ is the same quantity for the *RS,SR*2 isomer, etc., then the computed diastereoselective excess, de_{DFT}, is given by

$$de_{DFT} = (\langle E_{RS,SR}\rangle + \langle E_{RS,SR2}\rangle) - (\langle E_{RR,SS}\rangle + \langle E_{RR,SS2}\rangle) \quad (6)$$

Having identified the missing conformers with the combined MM−SEQM−DFT−MM approach, illustrated in Figure 7, it is possible that an MM-based de_{MM} will now compare more favorably with experimental de than reported earlier.[9] Unfortunately, the de_{MM} values are not in good agreement with experiment, even when the additional conformers are considered (Table 5). The internal energy differences between diastereomers that exhibit de = 0.90 is small (1.7 kcal/mol at 298.15 K), and molecular mechanics energies computed with the UFF are not sufficiently accurate to quantitatively predict experimental de values. Therefore, we must turn to the more accurate BOP/DNPP energies in order to obtain a computed diastereoselectivity that can be meaningfully compared to experiment.

With the exception of the *t*-Bu and $SiMe_3$ substituents, there is good agreement between de_{DFT} and experimental de (eq 6; Table 6). However, if we omit the additional conformers found after the MM grid search, then the agreement between computed and experimental de values is poor. For example, de_{DFT} for the Bn substituent increases from 0.806 with all conformers considered (Table 6) to 0.989 with only the lowest energy conformer for each of the four isomers (Table 2). The agreement between computed (0.801) and experimental de values (0.88) for the benzyl substituent is particularly remarkable, as Bn is often an outlier in comparisons between computed and experimental physical properties.[9,19]

The high computed de_{DFT} values for the *t*-Bu and $SiMe_3$ substituents are a consequence of the *RS,SR* isomers having a low BOP/DNPP energy and a low E''_R value. For both of these substituents, the high-energy, high-E''_R structures contain the substituent on the olefin displaced significantly from the C=C plane. For example, the average Re−C(*t*-Bu) distance is 3.64 Å for the high-energy isomers and 3.46 Å for the *RS,SR* isomer. Similarly, the average Re−Si distance is 3.94 Å for the high-energy isomers and 3.73 Å for the *RS,SR* isomer. Both the energies and the E''_R values for three of the four isomers are sufficiently large to force the Boltzmann weights to zero. Consequently, the diastereoselectivity is effectively based on a single conformer for the *t*-Bu and $SiMe_3$ substituents, whereas all other structures contain more than one competent conformer.

Ligand repulsive energies only consider the steric interaction between olefin and $[(\eta^5\text{-}C_5H_5)Re(NO)(PPh_3)]^+$ fragment. It is possible that there is an electronic effect that comes into play for the *t*-Bu and $SiMe_3$ substituents that accounts for the low experimental de values, which is under investigation in our laboratories.

Conclusions

A rigorous DFT approach to the stereoselective binding of prochiral α-olefins to $[(\eta^5\text{-}C_5H_5)Re(NO)(PPh_3)]^+$ has been undertaken. A new conformational search strategy has been developed that successively uses MM−SEQM−DFT−MM−DFT in order to locate all minima that can participate in a reaction. With all conformers identified, a computed diastereoselective excess, de_{DFT}, shows acceptable agreement with experiment for all olefins except the sterically bulky, electron-rich CH_2=CH(*t*-Bu) and CH_2=CH($SiMe_3$) olefins.

Acknowledgment. We thank the NSF (Grant No. CHE-0111131) for funding, the North Carolina Supercomputing Center (NCSC) for computer time, and Professor Tom Cundari, University of Memphis, and Dr. Lee Bartolotti, NCSC, for useful discussions.

OM020386H